IL-17A$^+$ γδT cell activation via the HMGB1-TLR2/4-NF-κB signaling pathways in biliary atresia

MENG-XIN ZHANG[1*], JING-FENG TANG[2*], MEI HONG[3*], YING YANG[4*], YUN ZHOU[1], SHUI-QING CHI[1], LI-YING RONG[1], GUO-QING CAO[1], XI ZHANG[1], JIN-XIANG ZHANG[2] and SHAO-TAO TANG[1]

[1]Department of Pediatric Surgery, Union Hospital, Tongji Medical College, Huazhong University of Science and Technology, Wuhan, Hubei 430019, P.R. China; [2]Department of Emergency Surgery, Union Hospital, Tongji Medical College, Huazhong University of Science and Technology, Wuhan, Hubei 430019, P.R. China; [3]Department of Thyroid Surgery, The First Affiliated Hospital, Zhejiang University School of Medicine, Hangzhou, Zhejiang 310003, P.R. China; [4]Department of Pediatric Surgery, Shanxi Children's Hospital, Taiyuan, Shanxi 030001, P.R. China

Received June 23, 2025; Accepted March 27, 2026

DOI: 10.3892/ijmm.2026.5852

Abstract. IL-17A$^+$ γδT cells are involved in biliary atresia (BA) inflammatory injury; however, the mechanism underlying their activation remains unclear. The present study aimed to elucidate the mechanism by which γδT cells are activated to secrete IL-17A in BA. Clinical samples from 27 patients with BA and 23 control individuals were collected and analyzed using reverse transcription-quantitative PCR (RT-qPCR), western blotting, ELISA, flow cytometry, Opal multiplex immunohistochemistry and immunohistochemistry. In addition, wild-type (WT) and *Tcrδ*$^{-/-}$ BA murine models were developed through infection with rhesus rotavirus (RRV) and assessed by RT-qPCR, western blotting, ELISA, flow cytometry, immunohistochemistry and hematoxylin and eosin staining. The release of high-mobility group box-1 (HMGB1) from RRV-infected biliary epithelial cells (BECs) and macrophages was investigated by ELISA and immunofluorescence confocal microscopy. In addition, co-culture systems of γδT cells with BECs or macrophages were established. The results revealed that the levels of hepatic IL-17A were higher in patients with BA, with γδT cells serving an important role in producing IL-17A. In the BA murine model, the IL-17A levels increased from day 3 to 14, and IL-17A$^+$ γδT cells peaked on day 7. The *Tcrδ*$^{-/-}$ BA murine model exhibited lower IL-17A levels, improved liver and bile duct morphology, and lower BA incidence compared with in the WT BA murine model, which was reversed through adoptive transfer of murine IL-17A$^+$ γδT cells. HMGB1, and Toll-like receptor (TLR)2 and 4 were upregulated in liver tissues from both patients with BA and the BA murine model. By contrast, hepatic IL-17A levels were decreased in the BA murine model treated with the HMGB1 inhibitor. In addition, HMGB1 was released from RRV-infected BECs or macrophages, and exogenous HMGB1 stimulation enhanced IL-17A production in γδT cells. The *Tlr2*$^{-/-}$ and *Tlr4*$^{-/-}$ γδT cell co-culture system inhibited IL-17A production and NF-κB activation, whereas NF-κB inhibition abolished HMGB1-induced IL-17A production in WT γδT cells. In conclusion, HMGB1 released from injured BECs or macrophages may activate IL-17A$^+$ γδT cells to mediate BA inflammatory injury via the HMGB1-TLR2/4-NF-κB pathways. The present study was registered with the Chinese Clinical Trial Registry (registration ID: ChiCTR2000039619; registered November 3, 2020).

Correspondence to: Professor Jin-Xiang Zhang, Department of Emergency Surgery, Union Hospital, Tongji Medical College, Huazhong University of Science and Technology, 1277 Jiefang Avenue, Wuhan, Hubei 430019, P.R. China
E-mail: zhangjinxiang@hust.edu.cn

Professor Shao-Tao Tang, Department of Pediatric Surgery, Union Hospital, Tongji Medical College, Huazhong University of Science and Technology, 1277 Jiefang Avenue, Wuhan, Hubei 430019, P.R. China
E-mail: tshaotao83@hust.edu.cn

*Contributed equally

Abbreviations: BA, biliary atresia; RRV, rhesus rotavirus; BECs, biliary epithelial cells; WT, wild-type; HMGB1, high-mobility group box-1; TLR, Toll-like receptor; DAMP, damage-associated molecular pattern; PAMP, pathogen-associated molecular pattern

Key words: BA, γδT cells, IL-17A, HMGB1, TLR2, TLR4

Introduction

The pathogenesis of biliary atresia (BA), which has not yet been fully elucidated, is multifactorial, involving genetic susceptibility, environmental influence and immune factors (1,2). Notably, virus-related autoimmune bile duct destruction is considered pivotal in BA pathogenesis (3). Several studies (4-6) have reported the presence of multiple immune cells in the hepatic portal region, which may be involved in the progression of hepatobiliary inflammation in BA.

Our previous study reported that the pro-inflammatory cytokine IL-17A is closely related to inflammation and

fibrosis in patients with BA (7). IL-17A has been shown to be upregulated in patients with BA and in experimental BA (7,8), whereas inhibiting IL-17A production can markedly reduce inflammation in experimental BA (9). Therefore, immune cells that produce IL-17A may be involved in the pathogenesis of BA. Several studies have indicated the critical involvement of IL-17A-producing γδT cells in targeting cholangiocyte damage in murine models of BA (9,10). Notably, γδT cells do not secrete IL-17A under steady-state conditions, and their activation, which is triggered by stress signals or other cytokine stimulation, is required for IL-17A secretion (9-11). However, the activation mechanism of IL-17A$^+$ γδT cells in BA remains unclear.

Extracellular high-mobility group box-1 (HMGB1) is released by various cells, including immune cells, and acts as a damage-associated molecular pattern (DAMP) molecule (12-14), mediating innate and adaptive immune responses. Aberrant activation of HMGB1 signaling can promote inflammation and autoimmune disorders (14,15). HMGB1 is upregulated in BA and thus may be involved in the pathogenesis of BA (13,14). Toll-like receptors (TLRs) can activate immune responses by recognizing and binding to corresponding pathogen-associated molecular patterns (PAMPs) and DAMPs (16,17). Extracellular HMGB1 can trigger early inflammatory and immune responses by binding with TLR2 and TLR4, and it is critical in multiple immunopathological processes (17,18). Moreover, hepatic TLR2 and TLR4 are upregulated in patients with BA and in a murine model of BA (19,20), which may trigger the classical downstream NF-κB pathway to mediate immune responses (21,22). However, it remains unclear as to whether HMGB1-TLR2/TLR4-NF-κB interaction activates γδT cells in BA. The present study aimed to investigate the mechanism underlying IL-17A$^+$ γδT-cell activation in BA.

Materials and methods

Human specimens. The present study was approved by the Ethics Committees of Union Hospital, Tongji Medical College (Wuhan, China; approval no. 2016-LSZ-S180) and Shanxi Children's Hospital (Taiyuan, China; approval no. 2RB-SB-2021-005), and was registered in the Chinese Clinical Trial Registry (registration ID: ChiCTR2000039619). Written informed consent was obtained from the guardians of all participants. Liver tissues were obtained from 27 patients with BA (BA group) undergoing Kasai portoenterostomy between May 2021 and December 2023, and from 23 age-matched patients with choledochal cyst undergoing surgery during the same period as the patients with BA. The BA group included 10 male patients and 17 female patients, with a median age at surgery of 54 days (range, 28-90 days), whereas the control group consisted of 8 male patients and 15 female patients, with a median age at surgery of 60 days (range, 25-98 days). Fresh liver samples were processed immediately after collection. Liver tissues for flow cytometry and magnetic bead-based cell enrichment were maintained on ice and utilized within 4 h, whereas the remaining samples were either fixed in 10% formalin (24 h at room temperature) for preparation of paraffin-embedded tissue sections or stored at -80˚C for mRNA isolation.

Mice. Adult wild-type (WT) Balb/c mice (n=48; 16 male mice and 32 female mice; age, 8-10 weeks; weight, 20-25 g) were purchased from Shulaibao (Wuhan) Biotechnology Co., Ltd. The *Tcrδ*$^{-/-}$, *Tlr2*$^{-/-}$ and *Tlr4*$^{-/-}$ Balb/c mice (n=2 male mice and 4 female mice per genotype; age, 8-10 weeks; weight, 20-25 g) were produced by Shanghai Model Organisms Center, Inc., using a proprietary CRISPR-Cas9 gene targeting platform. All mice were maintained in specific pathogen-free laminar-flow cages at a temperature of 23˚C and humidity of 50%, under a 12 h light/dark cycle with free access to standard chow and water. All procedures were approved by the Institutional Animal Care and Use Committee of Tongji Medical College, Huazhong University of Science and Technology (Wuhan, China; approval no. 4296; 2024). Experimental BA was induced in neonatal Balb/c mice (the WT offspring from the aforementioned adult WT mice; the *Tcrδ*$^{-/-}$ offspring from adult *Tcrδ*$^{-/-}$ mice; all mated in-house) by intraperitoneal injection of $1.5x10^6$ ffu rhesus rotavirus (RRV; provided by Professor C.L. Mack, University of Colorado, Denver, CO, USA) in 20 μl within 24 h of birth [n=25 for RRV group (11 male, 14 female); n=52 for *Tcrδ*$^{-/-}$ + RRV group (24 male, 28 female); n=54 for WT + RRV group (26 male, 28 female); n=48 for *Tcrδ*$^{-/-}$ + RRV + RPMI 1640 (cat. no. 11875093; Gibco; Thermo Fisher Scientific, Inc.) group (25 male, 23 female); n=51 for *Tcrδ*$^{-/-}$ + RRV + IL-17A$^+$ γδT group (24 male, 27 female)] (23), whereas control mice received minimum essential medium (MEM; cat. no. 11095080; Gibco; Thermo Fisher Scientific, Inc.) (n=25 for MEM group). Additionally, an independent cohort of neonatal WT mice (n=96; 45 male and 51 female; the offspring from the aforementioned adult WT mice) was used for γδT cell extraction following RRV injection. Separate cohorts of neonatal WT mice (n=18; 8 male and 10 female; the offspring from the aforementioned adult WT mice), *Tlr2*$^{-/-}$ mice (n=8; 4 male and 4 female; the offspring from the aforementioned adult *Tlr2*$^{-/-}$ mice), and *Tlr4*$^{-/-}$ mice (n=8; 5 male and 3 female; the offspring from the aforementioned adult *Tlr4*$^{-/-}$ mice) were used for γδT cell extraction. The mice were sacrificed on days 3, 7 and 14 for serum and tissue examination. Mice were anesthetized by intraperitoneal injection of sodium pentobarbital (70 mg/kg), followed by cardiac puncture for blood collection (50-150 μl per mouse). Subsequently, the mice were euthanized by cervical dislocation. Death was confirmed by the cessation of heartbeat and respiration, loss of reflexes and dilated pupils.

For inhibitor treatment, mice were intraperitoneally injected with glycyrrhizin (HMGB1 inhibitor; 50 mg/kg; cat. no. NSC 167409; Selleck Chemicals) on days 1, 3, 5 and 7 after RRV injection, respectively (n=20 for RRV + Glycyrrhizin group). The control group received an intraperitoneal injection of an equal volume of DMSO (n=20 for RRV + DMSO group). For macrophage depletion, mice were intraperitoneally administered with $GdCl_3$ (cat. no. G7532; Sigma-Aldrich; Merck KGaA) 24 h before RRV infection (n=15 for RRV + $GdCl_3$ group), whereas control mice were administered PBS (n=15 for RRV + PBS group).

Functional blockade assay. Mononuclear cells were isolated from the liver tissues of patients with BA (n=6) by density gradient centrifugation using Ficoll-Paque PLUS (cat. no. 17-1440-02; Cytiva) according to the manufacturer's

instructions. The cells were cultured in RPMI-1640 complete medium and stimulated with 1 μg/ml anti-CD3 monoclonal antibody (mAb; cat. no. 300437; BioLegend, Inc.) and 10 μg/ml anti-CD28 mAb (cat. no. 302933; BioLegend, Inc.) at 37˚C for 48 h. Subsequently, digoxin (100 nM; cat. no. S4290; Selleck Chemicals) or AM80 (100 nM; cat. no. 3507; Tocris Bioscience) was added to selectively inhibit T helper 17 (Th17) cells or γδT cells, respectively, followed by incubation at 37˚C for 72 h. Cell supernatants were then collected for IL-17A detection by ELISA.

Flow cytometry. Flow cytometry was performed using an LSRII cytometer (BioLegend, Inc.). Liver tissues from patients [BA group (n=5), control group (n=5)] and mice [MEM group (n=5 per time point), RRV group (n=5 per time point), RRV + DMSO group (n=5 per time point), RRV + Glycyrrhizin group (n=5 per time point)] were homogenized into single-cell suspensions and washed in PBS containing 0.3% fetal calf serum (FCS; cat. no. 10100147; Gibco; Thermo Fisher Scientific, Inc.) and 4 mM EDTA. Dead cells were stained with the LIVE/DEAD Fixable Aqua Dead Cell Staining kit (cat. no. L34957; Invitrogen; Thermo Fisher Scientific, Inc.) according to the manufacturer's protocol.

For extracellular staining at 4˚C for 30 min in the dark, human liver single cells were incubated with PE anti-human CD45 (cat. no. 368509), Alexa Fluor® 700 anti-human CD3 (cat. no. 300423), Brilliant Violet 421™ anti-human TCR γ/δ (cat. no. 331217) (all from BioLegend, Inc.), BB700 anti-human CD56 (cat. no. 566574; BD Biosciences), FITC anti-human CD4 (cat. no. 344604) and PE/Cyanine7 anti-human CD8 (cat. no. 344711) (both from BioLegend, Inc.). Th17 cells were identified as $CD3^+CD4^+$IL-$17A^+$ T cells.

Mouse liver single cells were incubated with APC/Cyanine7 anti-mouse CD45 (cat. no. 103115), Brilliant Violet 421™ anti-mouse CD3 (cat. no. 100227) and PE anti-mouse TCR γ/δ (cat. no. 118107) (all kits from BioLegend, Inc.).

For intracellular cytokine staining, the aforementioned human and mouse liver single cells were incubated for 2 h at 37˚C in MEM containing 5% FCS and Golgi Plug/Golgi Stop (cat. no. 554724; BD Biosciences). After fixation and permeabilization using the Cytofix/Cytoperm™ Fixation/Permeabilization kit (cat. no. 554714; BD Biosciences) according to the manufacturer's protocol, intracellular staining at 4˚C for 30 min in the dark was performed with APC anti-human IL-17A (cat. no. 512333) and Brilliant Violet 605™ anti-mouse IL-17A (cat. no. 506927) (both from BioLegend, Inc.). Analyses were performed using FlowJo v10.8.1 software (FlowJo; BD Biosciences).

Magnetic bead enrichment and stimulation of γδT cells. For magnetic bead enrichment, liver mononuclear cells from human [BA group (n=6)] and mouse [RRV-infected WT mice (n=96), WT mice (n=18), *Tlr2*$^{-/-}$ mice (n=8), *Tlr4*$^{-/-}$ mice (n=8)] liver tissues were used for γδT-cell enrichment. Because the yield of γδT cells from each neonatal mouse liver was limited, a relatively large number of RRV-infected WT mice was required to obtain sufficient viable γδT cells for subsequent *in vitro* cell experiments and adoptive-transfer experiments in the *Tcrδ*$^{-/-}$ + RRV + IL-$17A^+$ γδT group (n=51). By contrast, γδT cells isolated from WT mice, *Tlr2*$^{-/-}$ mice and *Tlr4*$^{-/-}$ mice were used only for *in vitro* co-culture experiments. Human BA samples were processed individually, whereas mouse liver mononuclear cells were pooled, when necessary, only within the same mouse group in each experimental batch. The cells from different mouse groups were not mixed with each other. The cells were separately incubated with biotinylated antibodies (biotin anti-human TCR γ/δ antibody, 1:100, cat. no. 331206; biotin anti-mouse TCR γ/δ antibody, 1:200, cat. no. 118103; both from BioLegend, Inc.) for 15 min at room temperature, followed by anti-biotin microbeads (20 μl per 10^7 cells; Miltenyi Biotec, Inc.) for 15 min at 4˚C and isolated through two rounds of magnetic separation using MS columns (designed for the positive selection of cells; Miltenyi Biotec, Inc.) to obtain γδT cells (live mononuclear cells, $CD3^+$ and TCR$γδ^+$). The purity of $CD3^+$ TCR$γδ^+$ cells isolated from liver tissues was >90% for both human and mouse samples (Fig. S1A and B). For activation of γδT cells from human and mouse liver tissues, subsets were separately stimulated with 10 ng/ml IL-1β (recombinant human IL-1β, cat. no. 579402; recombinant mouse IL-1β, cat. no. 575102; both from BioLegend, Inc.) and 10 ng/ml IL-23 (recombinant human IL-23, cat. no. 574102; recombinant mouse IL-23, cat. no. 589002; both from BioLegend, Inc.) at 37˚C for 48 h, and stimulated with 1 μg/ml anti-CD3 mAb (purified anti-human CD3, cat. no. 300437; purified anti-mouse CD3, cat. no. 100339; both from BioLegend, Inc.) and 10 μg/ml anti-CD28 mAb (purified anti-human CD28, cat. no. 302933; purified anti-mouse CD28, cat. no. 102115; both from BioLegend, Inc.) at 37˚C for 48 h.

Adoptive transfer of IL-17A$^+$ *γδT cells in vivo*. After RRV infection in neonatal *Tcrδ*$^{-/-}$ mice, 10^6 IL-$17A^+$ γδT cells isolated from RRV-infected WT mouse liver tissue, suspended in 50 μl RPMI 1640 medium (cat. no. 11875085; Gibco; Thermo Fisher Scientific, Inc.) were injected intraperitoneally within 24 h for 3 consecutive days. Control mice received medium alone and the relevant indexes were assessed: Hepatic IL-17A levels, liver histopathology, extrahepatic bile duct morphology, BA incidence, survival rate and hepatic pro-inflammatory cytokine levels.

HMGB1 stimulation. The purified human (n=3) γδT cells isolated from liver tissues were stimulated with HMGB1 (20 ng/ml; cat. no. 1690-HMB-050; R&D Systems, Inc.) for 48 h at 37˚C, then collected for flow cytometric analysis, whereas the supernatants were collected for IL-17A measurement.

RRV infection in BECs/macrophages and the co-culture system. All cells were cultured using RPMI 1640 medium containing 10% FCS, 2 mmol/l L-glutamine and 100 U/ml penicillin-streptomycin. Immortalized BECs were obtained from Shanghai Zhong Qiao Xin Zhou Biotechnology Co., Ltd., whereas THP-1 cells were purchased from Pricella®; Elabscience Bionovation, and were differentiated into macrophages with phorbol 12-myristate 13-acetate (cat. no. P8139; Sigma-Aldrich; Merck KGaA) at 37˚C for 24 h. RRV [multiplicity of infection (MOI)=20] was added to the culture medium of BECs and macrophages for incubation, and the release of HMGB1 was dynamically detected by immunofluorescence confocal microscopy in BECs, and by ELISA in the

supernatants of both BECs and macrophages after 0, 12, 24 and 36 h at 37˚C.

BECs or macrophages ($4x10^4$ cells/well) were cultured in 24-well plates. After placing the Transwell chamber (pore size, 0.4 μm; cat. no. 3470; Corning, Inc.) in a 24-well plate, 200 μl medium containing WT/*Tlr2*$^{-/-}$/*Tlr4*$^{-/-}$ γδT cells ($2x10^4$ cells/chamber) (isolated from the liver tissues of WT, *Tlr2*$^{-/-}$ or *Tlr4*$^{-/-}$ mice) was added to the chamber, along with anti-mouse CD3 mAb (1 μg/ml) and anti-mouse CD28 mAb (10 μg/ml), to establish a co-culture system. RRV (MOI=20) was added, whereas the control group received medium alone without RRV. Where indicated, WT γδT cells were pretreated with 10 μM Bay 11-7082 (NF-κB inhibitor; cat. no. S2913; Selleck Chemicals) for 1 h at 37˚C before co-culture. After 36 h of co-culture, the cell supernatant was collected for IL-17A detection.

Similarly, a co-culture system was established using BECs or macrophages with human γδT cells isolated from liver tissues of patients with BA (n=3). Briefly, BECs or macrophages ($4x10^4$ cells/well) were cultured in 24-well plates. Human γδT cells ($2x10^4$ cells/chamber) were added to the Transwell chamber (pore size, 0.4 μm), and stimulated with anti-human CD3 mAb (1 μg/ml) and anti-human CD28 mAb (10 μg/ml). Where specified, BECs or macrophages were pretreated with 40 μM glycyrrhizin for 2 h at 37˚C prior to co-culture, followed by the addition of RRV after co-culture establishment, with controls lacking RRV. After 36 h of co-culture, the IL-17A in the cell supernatant was detected.

Immunofluorescence confocal microscopy of HMGB1. BECs were immobilized using 4% paraformaldehyde for 30 min at room temperature, washed with PBS, and blocked with 3% bovine serum albumin (cat. no. BS114; Biosharp Life Sciences) at room temperature for 1 h. The cells were then incubated overnight with rabbit anti-HMGB1 antibody (1:800; cat. no. ab18256; Abcam) at 4˚C, followed by incubation with Cy3-conjugated goat anti-rabbit secondary antibody (1:100; cat. no. SA00009-2; Proteintech Group, Inc.) at room temperature for 1 h. After nuclear staining with DAPI at room temperature for 10 min, the cells were observed using a confocal fluorescence microscope (Olympus Corporation).

ELISA. Cell culture supernatants were collected and then centrifuged at 300 x g for 10 min at 4˚C to remove cellular debris, and the clarified supernatants were stored at -80˚C until detection. IL-17A and HMGB1 in liver homogenates [Humans: BA group (n=27), control group (n=23); Mice: MEM group (n=5 per time point), RRV group (n=5 per time point), WT + RRV group (n=5 per time point), *Tcrδ*$^{-/-}$ + RRV group (n=5 per time point), *Tcrδ*$^{-/-}$ + RRV + RPMI 1640 group (n=5 per time point), *Tcrδ*$^{-/-}$ + RRV + IL-17A$^+$ γδT group (n=5 per time point), RRV + DMSO group (n=5 per time point), RRV + Glycyrrhizin group (n=5 per time point), RRV + PBS group (n=5 per time point), RRV + $GdCl_3$ group (n=5 per time point)] and cell culture supernatants were detected according to the instructions of the IL-17A (cat. nos. ab216167 and ab199081; Abcam) and HMGB1 (cat. nos. SP14752 and SP11733; Wuhan Saipei Biotechnology Co., Ltd.) ELISA kits. A microplate reader (Spectramax Plus; Molecular Devices, LLC) was employed for plate analysis.

Opal multiplex immunohistochemistry. Liver tissue samples from patients [BA group (n=5), control group (n=5)] were fixed in 10% formalin at room temperature for 24 h, embedded in paraffin and cut into 4-μm sections. Slices of paraffin-embedded samples were prepared, followed by dewaxing with xylene, rehydration in graded alcohols and antigen restoration using EDTA at 95-100˚C for 20 min. The sections were sequentially stained with six primary antibodies (incubated at room temperature for 1 h) using the Opal seven-color immunohistochemistry detection kit (cat. no. NEL821001KT; PerkinElmer, Inc.) according to the manufacturer's instructions, followed by incubation with HRP-conjugated secondary antibodies (included in the Opal seven-color immunohistochemistry detection kit) at room temperature for 10 min and then DAPI nuclear staining. A tyramine signal amplification system was used after each round of primary antibody and HRP-conjugated secondary antibody staining, and antibody stripping was performed between each staining cycle according to the manufacturer's protocol. The primary antibodies and dyes were cytokeratin (CK)19 (1:400; cat. no. ab52625; Abcam)/green, CD3 (1:200; cat. no. A26443; ABclonal Biotech Co., Ltd.)/red, CD4 (1:600; cat. no. ab133616; Abcam)/magenta, IL-17A (1:200; cat. no. A12454; ABclonal Biotech Co., Ltd.)/cyan, NKG2D (1:1,000; cat. no. MA5-51623; Invitrogen; Thermo Fisher Scientific, Inc.)/grey and TCRγδ (1:500; cat. no. ab313573; Abcam)/yellow. The stained slides were scanned for panoramic imaging using a Vectra Polaris slide digital scanner (PerkinElmer, Inc.), and the results were evaluated by two pathologists.

RNA extraction and reverse transcription-quantitative PCR (RT-qPCR). Total RNA was isolated from human liver tissues [BA group (n=5-8), control group (n=5-8)], mouse liver tissues [MEM group (n=5), RRV group (n=5), WT + RRV group (n=5), *Tcrδ*$^{-/-}$ + RRV group (n=5), RRV + DMSO group (n=5), RRV + Glycyrrhizin group (n=5)] and γδT cells isolated from mouse liver using TRIzol® reagent (Invitrogen; Thermo Fisher Scientific, Inc.) and cDNA was synthesized using a PrimeScript™ RT Reagent Kit (Perfect Real Time; TaKaRa Bio, Inc.). The RT reaction was performed at 37˚C for 15 min, followed by inactivation at 85˚C for 5 sec. qPCR was performed with SYBR Green PCR Master Mix (SYBR Premix Ex Taq™ II; TaKaRa Bio, Inc.). The thermocycling program consisted of initial denaturation at 95˚C for 30 sec, followed by 40 cycles at 95˚C for 15 sec and 60˚C for 30 sec. The primer sequences are provided in Table SI. Transcript levels were normalized to GAPDH and were calculated via the $2^{-\Delta\Delta Cq}$ method (24).

Western blot analysis. Total proteins were extracted from human liver tissues [BA group (n=5-8), control group (n=5-8)], mouse liver tissues [MEM group (n=5), RRV group (n=5)] and γδT cells (isolated from mouse liver) using radioimmunoprecipitation assay lysis buffer (cat. no. P0013B; Beyotime Biotechnology) following the provided protocol. Protein concentrations were determined using a bicinchoninic acid protein assay kit (cat. no. P0010; Beyotime Biotechnology) according to the manufacturer's instructions. Equal amounts of total protein (20-30 μg/lane) were separated by SDS-PAGE on 10 or 12% gels, transferred onto polyvinylidene difluoride membranes, blocked with 5% fat-free milk at room temperature

for 45 min and incubated with the following primary antibodies overnight at 4˚C according to the recommended dilution method: Anti-IL17A rabbit polyclonal antibody (pAb) (1:2,000; cat. no. A12454; ABclonal Biotech Co., Ltd.), anti-HMGB1 rabbit pAb (1:5,000; cat. no. A2553; ABclonal Biotech Co., Ltd.), anti-TLR2 antibody (1:400; cat. no. ab213676; Abcam), anti-TLR4 antibody (1:10,000; cat. no. ab218987; Abcam), anti-NF-κB (1:10,000; cat. no. A19653; ABclonal Biotech Co., Ltd.), phosphorylated (p)-NF-κB p65/RelA-S536 rabbit mAb (1:10,000; cat. no. AP1294; ABclonal Biotech Co., Ltd.) and anti-GAPDH mAb (1:50,000; cat. no. 60004-1-Ig; Proteintech Group, Inc.). Subsequently, the membranes were incubated with horseradish peroxidase-conjugated secondary antibodies for 1 h at room temperature (anti-rabbit IgG: 1:5,000; cat. no. RGAR001; anti-mouse IgG: 1:5,000; cat. no. RGAM001; both from Proteintech Group, Inc.). Proteins were visualized with enhanced chemiluminescence detection reagent (cat. no. RM00020P; ABclonal Biotech Co., Ltd.).

Immunohistochemistry and hematoxylin and eosin (H&E) staining. Briefly, human [BA group (n=8), control group (n=8)] and mouse liver tissues [MEM group (n=5), RRV group (n=5), WT + RRV group (n=5), *Tcrδ*$^{-/-}$ + RRV group (n=5), *Tcrδ*$^{-/-}$ + RRV + RPMI 1640 group (n=5), *Tcrδ*$^{-/-}$ + RRV + IL-17A^{+} γδT group (n=5), RRV + DMSO group (n=5), RRV + Glycyrrhizin group (n=5)] were fixed in 10% formalin at room temperature for 24 h, followed by paraffin embedding and sectioning. The paraffin-embedded sections (4 μm) were dewaxed using xylene and rehydrated in graded alcohols. After antigen retrieval using either sodium citrate buffer or EDTA at a temperature of 95-100˚C for 20 min continuously, endogenous enzyme blocking was performed with 3% H_2O_2 for 10 min at room temperature and then 5% goat serum (cat. no. C0265; Beyotime Biotechnology) was used for blocking (at room temperature for 30 min). According to the manufacturer's instructions, the sections were then incubated with the following primary antibodies overnight at 4˚C: Anti-CK19 antibody (1:400; cat. no. ab52625; Abcam), anti-HMGB1 rabbit pAb (1:100; cat. no. A2553; ABclonal Biotech Co., Ltd.), anti-TLR2 antibody (1:200; cat. no. ab213676; Abcam) and anti-TLR4 antibody (1:200; cat. no. ab218987; Abcam), followed by incubation with secondary antibody (HRP-conjugated goat anti-rabbit IgG; 1:50; cat. no. A0208; Beyotime Biotechnology) for 1 h at room temperature. After DAB solution was added for color development, the sections were counterstained with hematoxylin for 1 min at room temperature. In addition, some paraffin-embedded sections underwent H&E staining, using 0.5% hematoxylin for 5 min at room temperature and 0.05% eosin for 1 min at room temperature. All stained sections were observed using a light microscope (Nikon Corporation). The results were assessed by two pathologists.

Statistical analysis. Data were analyzed using FlowJo software (v10.8.1) and GraphPad Prism 8.0 software (Dotmatics). The χ^2 test was used to compare the BA incidence between two groups. Continuous data between two groups were compared using the unpaired Student's t-test, whereas comparisons across three or more groups were performed using one-way ANOVA, followed by Bonferroni's post hoc test for pairwise comparisons. All experiments were performed in triplicate. Following intraperitoneal injections of RRV or saline within 24 h after birth, the survival and disease status of neonatal mice [n=28 for *Tcrδ*$^{-/-}$ + RRV group; n=34 for WT + RRV group; n=32 for *Tcrδ*$^{-/-}$ + RRV + RPMI 1640 group; n=34 for *Tcrδ*$^{-/-}$ + RRV + IL-17A^{+} γδT group] were assessed and recorded for 20 consecutive days. Day 1 was regarded as the starting point, and the event of death as the endpoint. Survival curves were generated using the Kaplan-Meier method and compared using the log-rank test. The hazard ratio (HR) with a 95% confidence interval (CI) was calculated as part of the log-rank analysis. $P<0.05$ was considered to indicate a statistically significant difference.

Results

IL-17A serves an important role in the inflammatory injury of patients with BA and is produced by γδT cells. IL-17A is a key pathogenic cytokine in various inflammatory and autoimmune processes (10,22). In the present study, hepatic IL-17A levels were measured using RT-qPCR (Fig. 1A), western blotting (Fig. 1B) and ELISA (Fig. 1C) to investigate its role in BA; the results revealed that IL-17A levels were higher in the BA group compared with those in the control group. Flow cytometric analysis of human liver tissues identified TCRγδ^{+} T cells (γδT cells), CD56^{+} T cells (natural killer T cells), CD4^{+} T cells and CD8^{+} T cells as potential IL-17A sources (Fig. 1D), with CD4^{+}IL-17A^{+} T cells (Th17 cells) and IL-17A^{+} γδT cells showing the highest increases in percentages within their respective subsets (Fig. 1D and E). In Fig. 1E, quantitative analysis of the percentages represent the proportion of IL-17A^{+} cells within their respective T cell subsets (for example, CD56^{+} IL-17A^{+} T cells/CD56^{+} T cells), calculated as [(upper-right quadrant)/(upper-right + lower-right quadrants) x100%] based on the flow cytometry dot plots in Fig. 1D. Opal multiplex immunohistochemistry results revealed that the BA group had higher levels of CK19 markers in the liver, indicating abnormal proliferation of intrahepatic bile ducts, and IL-17A, NKG2D immune activation index, CD3, CD4 and TCRγδ were markedly increased around the bile ducts (Fig. 1F). Quantitative analysis validated higher percentages of IL-17A^{+} γδT cells in γδT cells and Th17 cells in CD4^{+} T cells in BA (Fig. 1G), which was consistent with the flow cytometry results. Functional blockade experiments using digoxin (Th17 cell inhibitor) and AM80 (γδT cell inhibitor) on mononuclear cells isolated from the liver tissues of patients with BA demonstrated γδT cells as an important source of IL-17A, with AM80 treatment causing a more marked reduction in IL-17A levels (Fig. 1H). These results indicated that γδT cells are the major producers of IL-17A driving inflammatory injury in BA, consistent with previous study results (9,10).

IL-17A^{+} γδT cells induce the inflammatory response in the BA model. A mouse model of BA was established to elucidate the role of IL-17A^{+} γδT cells in BA progression. Dynamic analysis revealed a time-dependent increase in IL-17A levels in liver homogenate supernatants from day 3 to 14 (Fig. 2A), whereas the proportion of IL-17A^{+} γδT cells in the liver tissue increased from day 3 and peaked at day 7 (Figs. 2B and S1C), suggesting their pathogenic role in initiating an early inflammatory response in BA. The murine BA model on day 7 was used

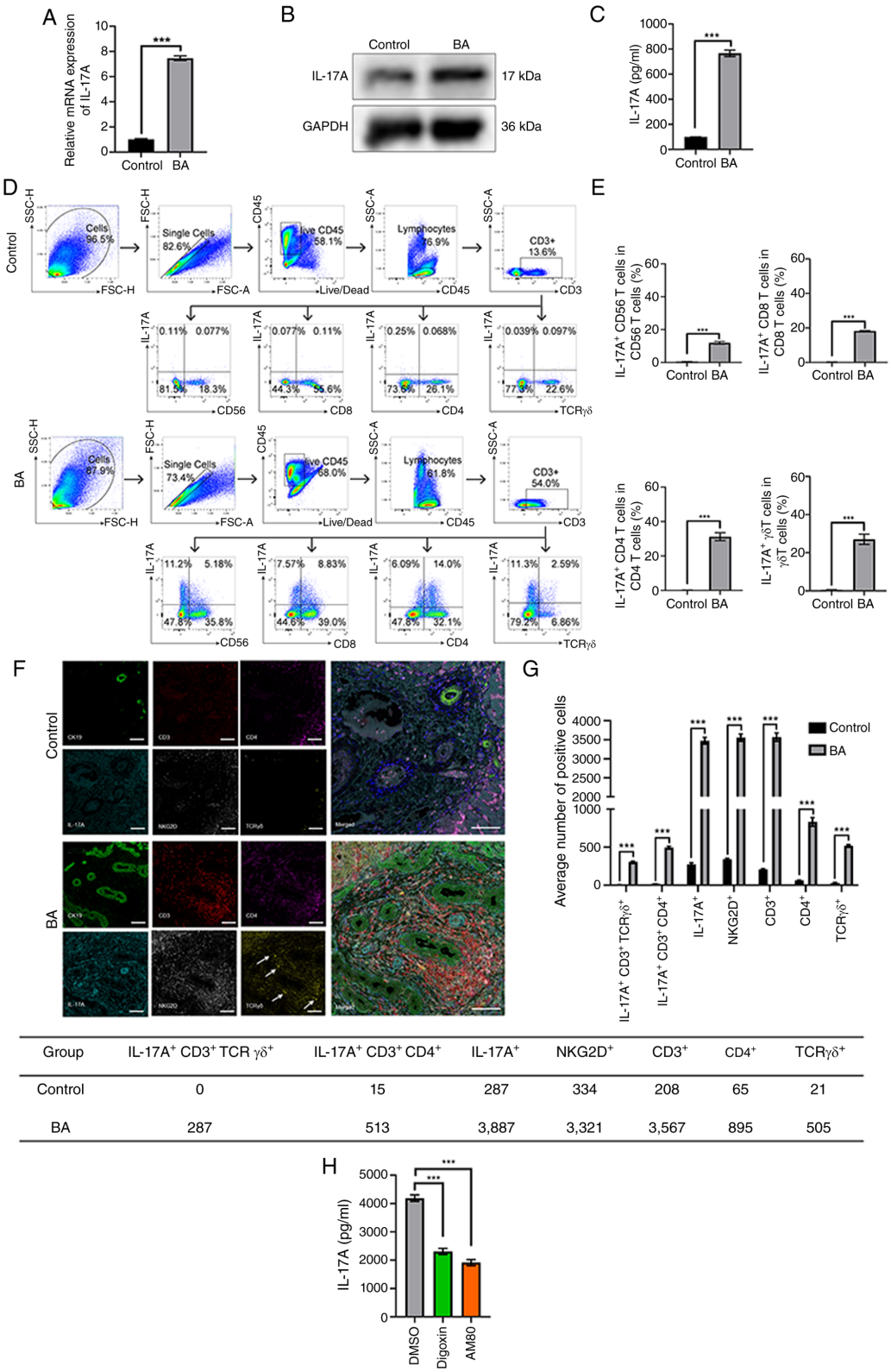

Group	IL-17A$^+$ CD3$^+$ TCR γδ$^+$	IL-17A$^+$ CD3$^+$ CD4$^+$	IL-17A$^+$	NKG2D$^+$	CD3$^+$	CD4$^+$	TCRγδ$^+$
Control	0	15	287	334	208	65	21
BA	287	513	3,887	3,321	3,567	895	505

Figure 1. IL-17A is highly expressed in the liver tissues of patients with BA and γδT cells are major producers of IL-17A. (A) Reverse transcription-quantitative PCR was used to quantify the mRNA levels of IL-17A relative to GAPDH, revealing increased mRNA levels of IL-17A in the liver of patients with BA (n=5/group). (B) Western blotting (n=5/group) and (C) ELISA (n=27 for BA group, n=23 for control group) showed higher IL-17A protein levels in the liver of patients with BA. (D and E) Single cell suspensions were prepared from the liver tissue of patients with BA and control individuals, followed by extracellular and intracellular staining. (D) Representative flow cytometry plots showing the gating strategy for IL-17A$^+$ CD56$^+$ T cells, IL-17A$^+$ CD8$^+$ T cells, IL-17A$^+$ CD4$^+$ T cells (Th17 cells) and IL-17A$^+$ γδT cells (n=5/group). (E) Percentage of IL-17A$^+$ subsets in CD56$^+$, CD8$^+$, CD4$^+$ and TCRγδ$^+$ T cells (n=5/group). (F) Representative images of the localization of CK19, IL-17A, CD3, CD4, TCRγδ and NKG2D expression in liver tissue, as detected through Opal multiplex immunohistochemistry (n=5/group). Scale bar, 50 μm. (G) Quantitative analysis of IL-17A$^+$ CD3$^+$ TCRγδ$^+$, IL-17A$^+$ CD3$^+$ CD4$^+$, IL-17A$^+$, NKG2D$^+$, CD3$^+$, CD4$^+$ and TCRγδ$^+$ cells, as determined using Opal multiplex immunohistochemistry (n=5/group). (H) After adding anti-CD3 mAb and anti-CD28 mAb to liver mononuclear cells from patients with BA (n=6), the secretion of IL-17A by Th17 cells and γδT cells was inhibited by digoxin and AM80, respectively. The concentration of IL-17A in the cell supernatant was subsequently detected by ELISA. Data are presented as the mean ± standard deviation of at least three repeated experiments. ***P<0.001. BA, biliary atresia; CK19, cytokeratin 19; mAb, monoclonal antibody; Th17, T helper 17.

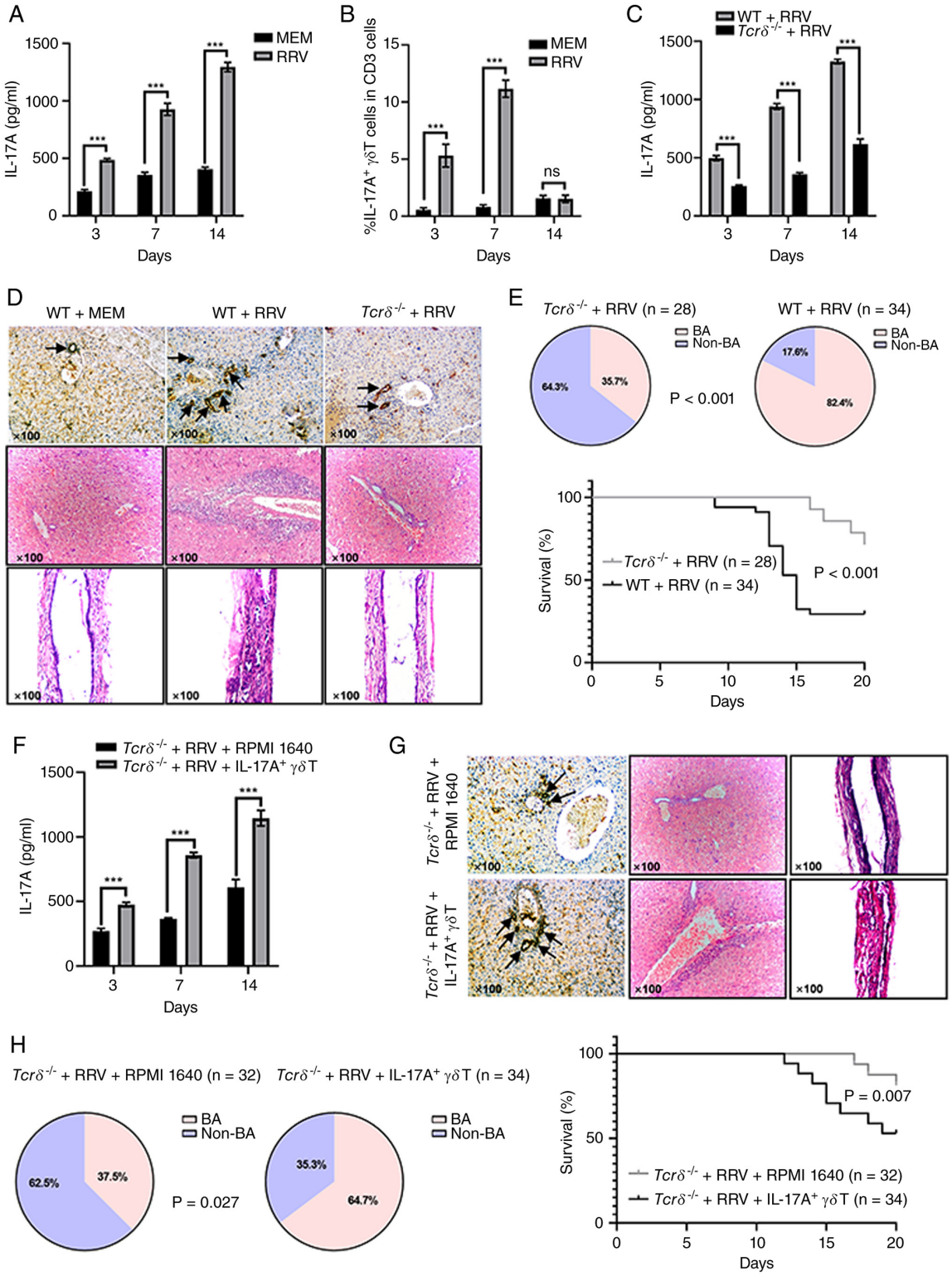

Figure 2. IL-17A$^+$ γδT cells are increased and induce the inflammatory response in experimental BA. Experimental BA was induced in neonatal Balb/c mice through intraperitoneal injection of RRV; after RRV injection, (A) IL-17A levels in the liver homogenate supernatant of the murine BA model were dynamically measured through ELISA (n=5/group per time point), and (B) IL-17A$^+$ γδT cells were dynamically analyzed through flow cytometry on days 3, 7 and 14 (n=5/group per time point). (C) After knocking out the *Tcrδ* gene in Balb/c mice, the dynamic change in IL-17A content in the liver tissue of the *Tcrδ*$^{-/-}$ murine BA model was measured through ELISA (n=5/group per time point). (D) On day 7 of the *Tcrδ*$^{-/-}$ murine BA model, immunohistochemical staining with CK19 (upper panels, original magnification, x100) was used to observe the morphology of intrahepatic bile ducts, and H&E staining (original magnification, x100) was used to observe liver inflammation (middle panels) and extrahepatic bile duct morphology (lower panels) (n=5/group). (E) Incidence of BA and survival analysis in the *Tcrδ*$^{-/-}$ murine BA model (n=28 for *Tcrδ*$^{-/-}$ + RRV group, n=34 for WT + RRV group). (F-H) After adoptive transfusion of murine IL-17A$^+$ γδT cells into *Tcrδ*$^{-/-}$ mice, the aforementioned indicators were observed. (F) Dynamic changes in hepatic IL-17A levels were measured by ELISA (n=5/group per time point). (G) Liver inflammation, intrahepatic bile duct morphology and extrahepatic bile duct morphology were analyzed by immunohistochemical staining with CK19 (left panels, original magnification, x100) and H&E staining (middle panels for liver inflammation and right panels for extrahepatic bile duct morphology, original magnification, x100) (n=5/group). (H) Incidence of BA and survival analysis (n=32 for *Tcrδ*$^{-/-}$ + RRV + RPMI 1640 group, n=34 for *Tcrδ*$^{-/-}$ + RRV + IL-17A$^+$ γδT group). Data are presented as the mean ± standard deviation of at least three repeated experiments. ***P<0.001; ns, not significant. BA, biliary atresia; CK19, cytokeratin 19; H&E, hematoxylin and eosin; MEM, minimum essential medium; RRV, rhesus rotavirus; WT, wild-type.

for further analysis. Mice with BA exhibited elevated hepatic mRNA levels of IL-1β, IL-6 and TNF-α compared with those in the control group (Fig. S2A), reflecting a pro-inflammatory state. Moreover, compared with in the WT murine model of BA, the *Tcrδ*$^{-/-}$ murine model of BA exhibited reduced hepatic IL-17A levels (a 61.89% reduction at day 7; Fig. 2C), improved liver inflammation, reduced intrahepatic bile duct proliferation and improved extrahepatic bile ducts (Fig. 2D). The incidence of BA was markedly decreased from 82.4% (28/34) in WT mice to 35.7% (10/28) in *Tcrδ*$^{-/-}$ mice (Fig. 2E), with a concomitant increase in 20-day survival rate from 29.4% (10/34) to 71.4% (20/28) [HR for WT vs. *Tcrδ*$^{-/-}$=4.147; 95% CI, 2.055-8.369; Fig. 2E]. Concomitant reductions in IL-1β, IL-6 and TNF-α in *Tcrδ*$^{-/-}$ mice compared with in WT mice further validated the role of IL-17A$^+$ γδT in orchestrating inflammatory responses (Fig. S2B). By contrast, adoptive transfusion of IL-17A$^+$ γδT cells into the *Tcrδ*$^{-/-}$ murine BA model (n=34) notably exacerbated these parameters compared with in the *Tcrδ*$^{-/-}$ murine BA model receiving RPMI-1640 medium (n=32) (Fig. 2F-H). These data indicated that γδT cell-derived IL-17A may be critical for BA progression.

HMGB1 is essential to activate IL-17A$^+$ γδT cells. HMGB1, as a DAMP, triggers early inflammatory responses in various pathologies and is important in the pathogenesis of BA (12,13). Therefore, the expression of HMGB1 in BA and its role in IL-17A$^+$ γδT cell activation were explored in the present study. Immunohistochemical staining results showed elevated HMGB1 expression in the hepatic portal area of patients with BA and in the BA mouse model (Fig. 3A and B). Similarly, the mRNA and protein expression levels of HMGB1 were markedly higher in BA (Fig. 3C-F). After inhibiting HMGB1 with glycyrrhizin, the BA mouse model showed a significant decrease in the proportion of hepatic IL-17A$^+$ γδT cells and IL-17A levels in the liver homogenate supernatant on days 3 and 7 (Figs. 3G, H and S1D). Meanwhile, compared with that in the untreated BA mice, HMGB1 inhibition reduced pro-inflammatory cytokine levels (IL-1β, IL-6 and TNF-α; Fig. S2C), which is consistent with the role of HMGB1 in BA hepatic inflammation. These changes were accompanied by improvements in liver inflammation, intrahepatic bile duct proliferation and extrahepatic bile duct obstruction (Fig. 3I). These results suggested that HMGB1 may be critical in IL-17A production by γδT cells in BA. Subsequently, 48-h exogenous HMGB1 *in vitro* stimulation of hepatic γδT cells from patients with BA increased the percentage of IL-17A$^+$ γδT cells (Figs. 3J and S1E) and IL-17A levels (Fig. 3K), further demonstrating the importance of HMGB1 in IL-17A$^+$ γδT cell activation.

HMGB1 is released from BECs and macrophages in response to RRV infection and promotes IL-17A secretion by γδT cells. To determine the cellular sources of HMGB1 in BA, the present study continued to focus on BECs and macrophages, which are known targets of RRV infection that have a key role in hepatic inflammation (13,20). The capacity of BECs or macrophages to release HMGB1 after RRV infection was explored *in vitro* to validate their role in HMGB1 production. The immunofluorescence confocal assay (Fig. 4A) showed that HMGB1 protein was located in the nucleus of BECs at 0 h of RRV infection and began to be released from the nucleus at 12 h. A large amount of nuclear HMGB1 was accumulated in the cytoplasm and extracellular areas of BECs at 24 and 36 h. Meanwhile, the observed low nuclear signals of HMGB1 at 24 and 36 h likely reflect that the rate of HMGB1 release exceeds that of its synthesis, resulting in a reduction in nuclear HMGB1 staining. Correspondingly, BEC supernatants had higher HMGB1 levels at 24 and 36 h after RRV infection (Fig. 4B). Similar findings were observed in macrophages (Fig. 4C), suggesting both BECs and macrophages contribute to HMGB1 release in BA. Consistent with previous studies, HMGB1 was actively released from BECs after RRV infection in the experimental BA model (13,25). *In vivo*, macrophage depletion via $GdCl_3$ reduced serum HMGB1 at days 7 and 14 (Fig. 4D), and hepatic IL-17A concentrations at days 3 and 7 (Fig. 4E) in the BA murine model, confirming macrophages as important sources of HMGB1.

Subsequently, the present study investigated whether HMGB1 directly participated in γδT cell activation. BECs and macrophages were co-cultured with γδT cells derived from patients with BA, and IL-17A levels in the cell supernatant were measured under the intervention of RRV and glycyrrhizin (HMGB1 inhibitor) separately or in combination (Fig. 4F). Co-culture of RRV-infected BECs or macrophages with γδT cells derived from patients with BA significantly increased IL-17A secretion compared with co-culture with BECs or macrophages uninfected with RRV, which was suppressed by pre-incubating BECs or macrophages with glycyrrhizin (HMGB1 inhibitor) before co-culture (Fig. 4F).

HMGB1-TLR2/4-NF-κB signaling axis mediates the activation of the IL-17A$^+$ γδT cells. Due to the interaction of HMGB1 with TLRs on various cell surfaces, including TLR2 and TLR4 (20,26), and the importance of TLR2 and TLR4 in γδT cell activation (27), the present study aimed to verify whether HMGB1 activates γδT cells through the TLR2/4-NF-κB pathways. The expression levels of TLR2 and TLR4 were notably upregulated in patients with BA (Fig. 5A-C) and localized near the hepatic portal area (Fig. 5C), indicating activation of the TLR2 and TLR4 pathways. In addition, the BA murine model showed similar findings, with higher expression of TLR2 and TLR4 compared with in control mice receiving MEM (Fig. 5D-F). The extraction of γδT cells from human liver tissues in the control group was insufficient, making it difficult to detect TLR2 and TLR4 on these cells. Therefore, the present study investigated the TLR pathway in γδT cells in the BA murine model, and the results showed higher mRNA and protein levels of TLR2 and TLR4 in IL-17A$^+$ γδT cells compared with in γδT cells (Fig. 5G and H).

To further demonstrate the effect of TLR2 and TLR4 pathways on γδT cell activation, γδT cells were extracted from WT, *Tlr2*$^{-/-}$ and *Tlr4*$^{-/-}$ mice, and were co-cultured with RRV-infected BECs or macrophages *in vitro*. After stimulation with RRV for 36 h, the IL-17A secretion levels of the *Tlr2*$^{-/-}$ and *Tlr4*$^{-/-}$ γδT cells were significantly lower than those of WT γδT cells (Fig. 6A and B). These findings indicated the importance of TLR2 and TLR4 on γδT cells in IL-17A secretion. The reduced IL-17A production by *Tlr2*$^{-/-}$ and *Tlr4*$^{-/-}$ γδT cells in co-culture with RRV-infected BECs or macrophages (releasing HMGB1) confirms that the HMGB1-TLR2/4 pathways mediates IL-17A$^+$ γδT cell activation.

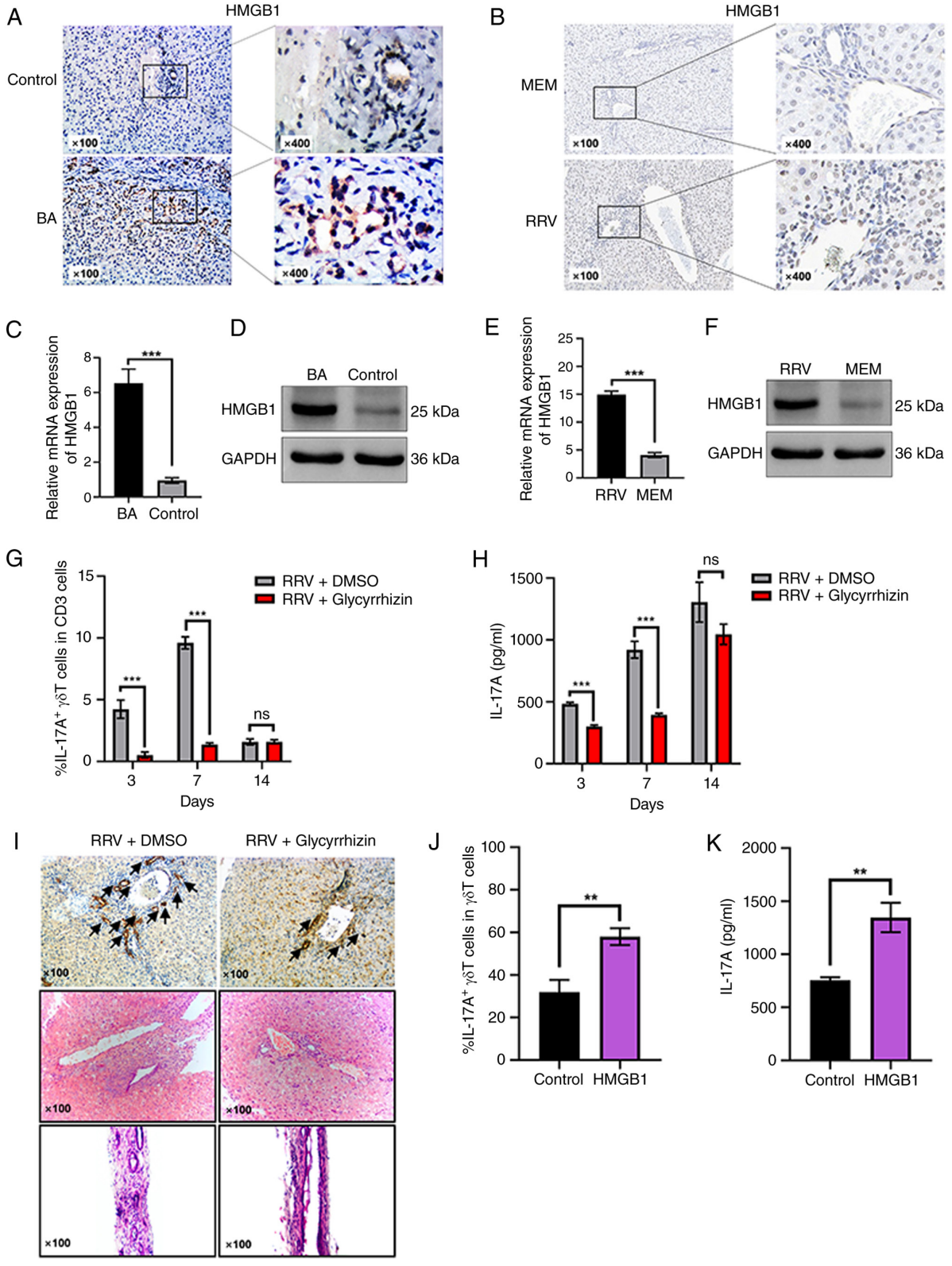

Figure 3. HMGB1 is essential for activation of IL-17A$^+$ γδT cells in BA. Representative immunohistochemical staining of increased HMGB1 expression in the liver tissues of (A) patients with BA (n=8/group) and (B) the BA murine model on day 7 (n=5/group) (original magnification, x100 and x400). Increased (C) mRNA (n=8/group) and (D) protein expression levels (n=8/group) of HMGB1 in patients with BA, and increased (E) mRNA and (F) protein expression levels of HMGB1 in experimental BA on day 7 were measured through reverse transcription-quantitative PCR (n=5/group) and western blotting (n=5/group). mRNA levels were normalized to GAPDH levels. After inhibition of HMGB1 with glycyrrhizin, (G) reduced proportions of IL-17A$^+$ γδT cells were detected through flow cytometry (n=5/group per time point) and (H) lower IL-17A levels were measured by ELISA (n=5/group per time point) in the liver tissues of the murine BA model on days 3, 7 and 14. (I) Immunohistochemical staining with cytokeratin 19 (upper panels) and hematoxylin and eosin staining (middle panels for liver inflammation and lower panels for extrahepatic bile duct morphology) for improvements in liver inflammation, and intrahepatic and extrahepatic bile duct obstruction of the murine BA model on day 7 (n=5/group, original magnification, x100). After stimulation of hepatic γδT cells of patients with BA with HMGB1 *in vitro*, the (J) percentage of IL-17A$^+$ γδT cells was detected through flow cytometry (n=3) and (K) IL-17A levels in the cell supernatant were measured through ELISA (n=3). Data are presented as the mean ± standard deviation of at least three repeated experiments. **P<0.01. ***P<0.001; ns, not significant. BA, biliary atresia; HMGB1, high-mobility group box-1; MEM, minimum essential medium; RRV, rhesus rotavirus.

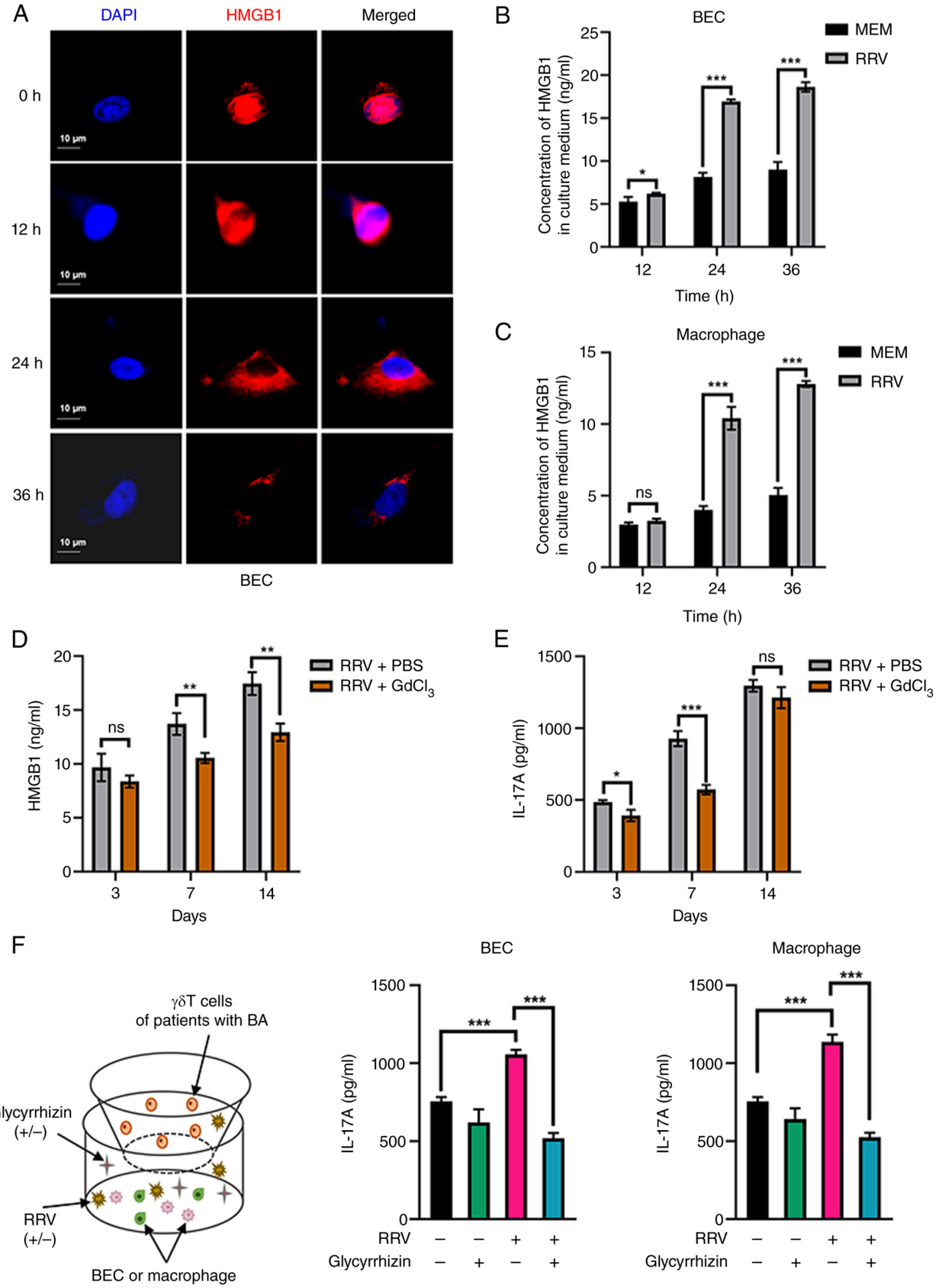

Figure 4. After RRV infection, HMGB1 is released from BECs and macrophages, and promotes IL-17A secretion by γδT cells. (A) In an immunofluorescence confocal assay, HMGB1 was released from the nucleus of BECs at different time points (0, 12, 24 and 36 h) following RRV infection. The nucleus was stained blue and HMGB1 was stained red. Scale bar, 10 μm. The secretion of HMGB1 in the cell supernatant of (B) BECs and (C) macrophages stimulated by RRV was dynamically measured through ELISA. After macrophage depletion using $GdCl_3$, (D) serum HMGB1 (n=5/group per time point) and (E) liver IL-17A levels (n=5/group per time point) were detected through ELISA. (F) A co-culture system of BECs or macrophages and γδT cells of patients with BA (n=3) was established. IL-17A levels in the supernatant of the co-culture system were measured by ELISA after the intervention of BECs or macrophages with RRV, as well as pretreatment with glycyrrhizin before co-culture. Data are presented as the mean ± of at least three repeated experiments. *P<0.05, **P<0.01, ***P<0.001; ns, not significant. BA, biliary atresia; BEC, biliary epithelial cell; HMGB1, high-mobility group box-1; MEM, minimum essential medium; RRV, rhesus rotavirus.

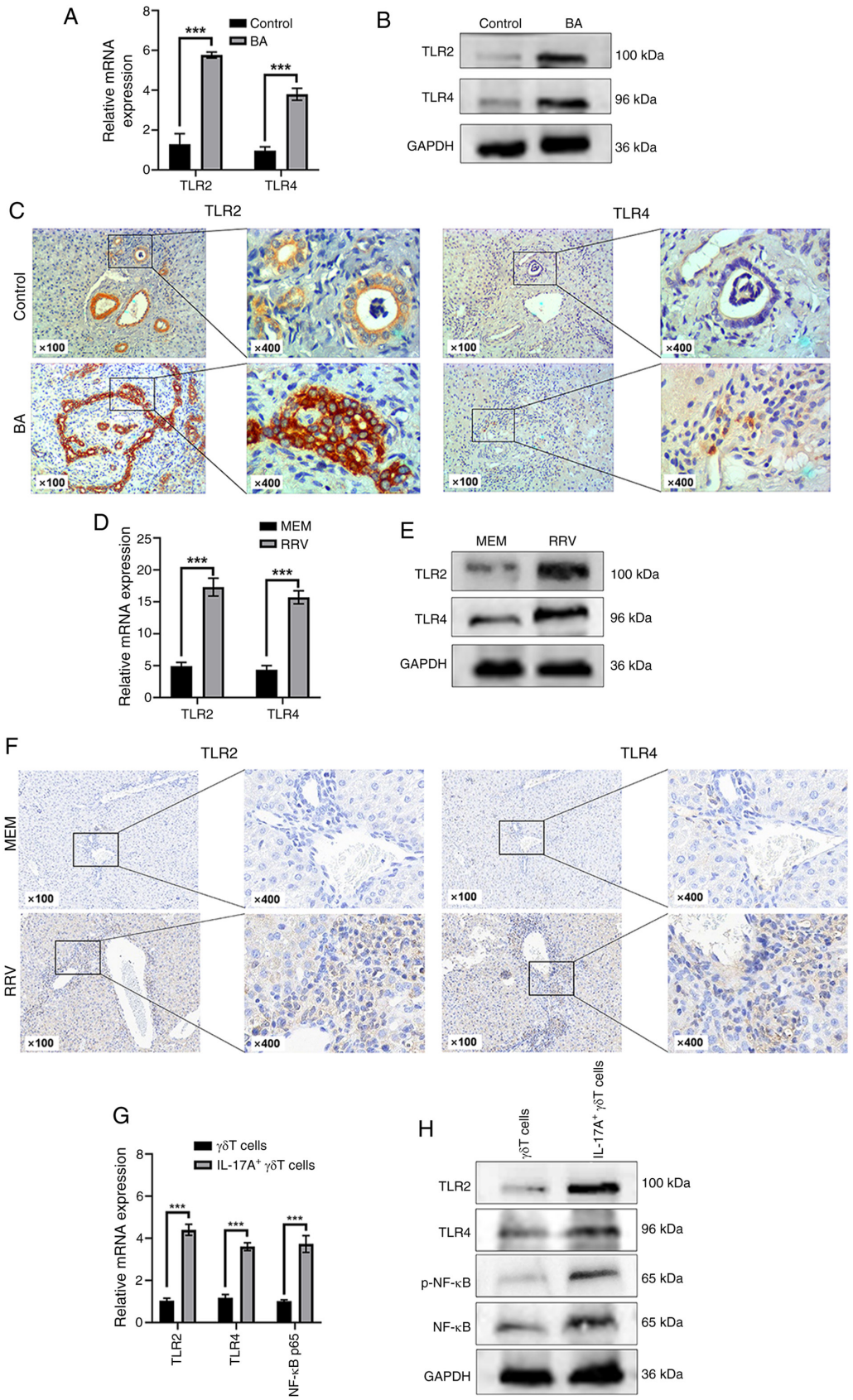

Figure 5. TLR2 and TLR4 are highly expressed in the liver tissues of humans and experimental BA. TLR2 and TLR4 expression in liver tissues was detected through (A) RT-qPCR (n=8/group), (B) western blotting (n=8/group) and (C) immunohistochemical staining (n=8/group, original magnification, x100 and x400), with higher mRNA and protein levels detected in patients with BA. TLR2 and TLR4 expression was detected in the experimental BA model on day 7 (n=5/group) by (D) RT-qPCR, (E) western blotting and (F) immunohistochemical staining (original magnification, x100 and x400). RT-qPCR data were normalized to GAPDH. Expression of TLR2, TLR4 and NF-κB on hepatic IL-17A$^+$ γδT cells in the BA murine model on day 7 (n=5/group) was detected through (G) RT-qPCR and (H) western blotting. Data are presented as the mean ± standard deviation of at least three repeated experiments. ***P<0.001. BA, biliary atresia; MEM, minimum essential medium; p-, phosphorylated; RRV, rhesus rotavirus; RT-qPCR, reverse transcription-quantitative PCR; TLR, Toll-like receptor.

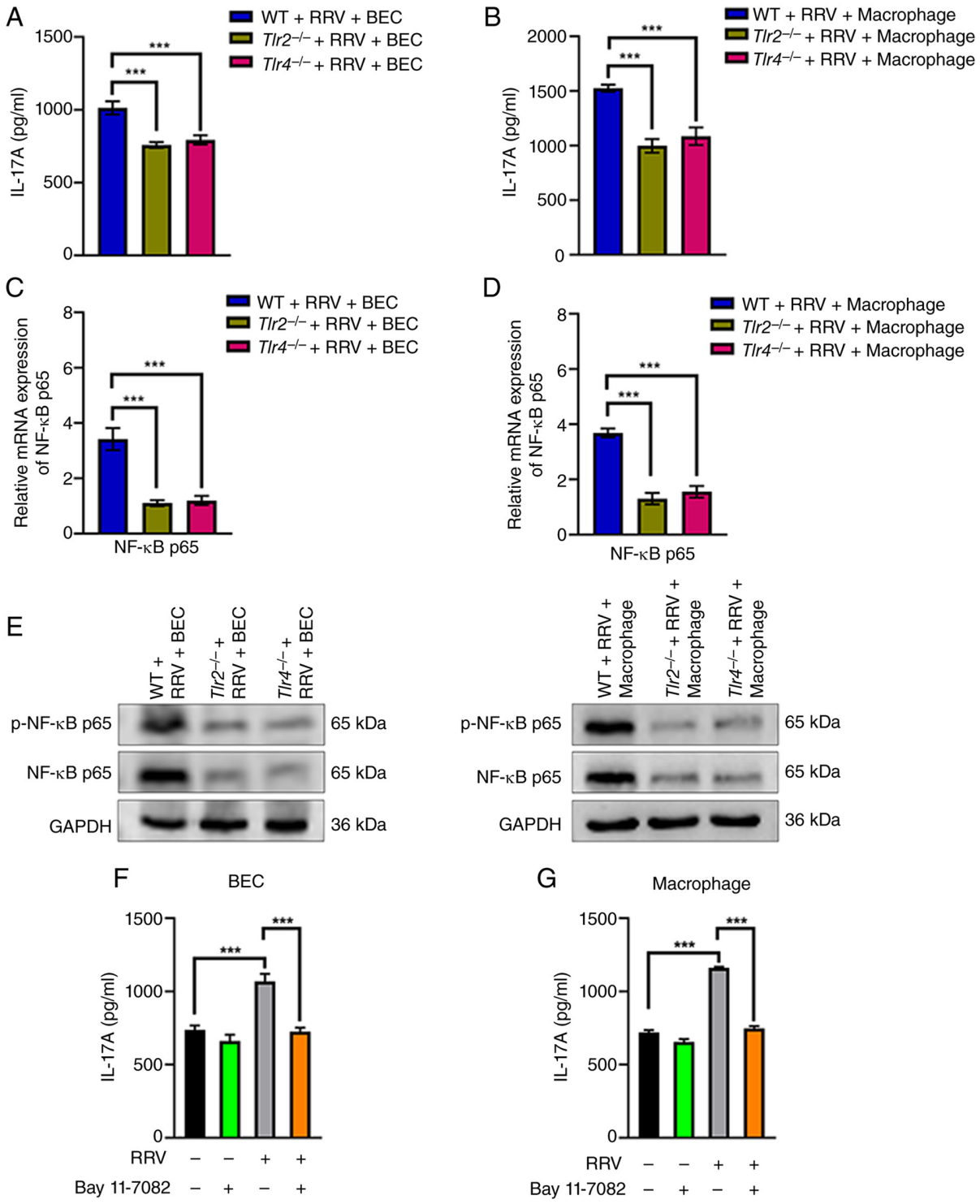

Figure 6. Roles of TLR2/TLR4-NF-κB in the activation of IL-17A$^+$ γδT cells by HMGB1. After establishing the co-culture system of γδT cells from WT, *Tlr2*$^{-/-}$ and *Tlr4*$^{-/-}$ mice with (A) BECs or (B) macrophages *in vitro*, the IL-17A levels in the supernatant of the co-culture system were measured through ELISA under the stimulation of RRV. After co-culture of WT, *Tlr2*$^{-/-}$ or *Tlr4*$^{-/-}$ γδT cells with RRV-stimulated BECs or macrophages, the NF-κB p65 and p-NF-κB p65 expression levels were measured. The mRNA levels of NF-κB in WT, *Tlr2*$^{-/-}$ or *Tlr4*$^{-/-}$ γδT cells were detected by reverse transcription-quantitative PCR after co-culture with RRV-stimulated (C) BECs or (D) macrophages. NF-κB p65 and p-NF-κB p65 protein expression levels in WT, *Tlr2*$^{-/-}$ or *Tlr4*$^{-/-}$ γδT cells were analyzed by western blotting after co-culture with RRV-stimulated (E) BECs (left panel) or macrophages (right panel). Detection of IL-17A levels after pretreatment with the NF-κB inhibitor Bay 11-7082 in WT γδT cells, followed by co-culture with (F) BECs or (G) macrophages, which secrete HMGB1 after RRV infection. Data are presented as the mean ± standard deviation of at least three repeated experiments. ***P<0.001. BEC, biliary epithelial cell; HMGB1, high-mobility group box-1; p-, phosphorylated; RRV, rhesus rotavirus; TLR, Toll-like receptor; WT, wild-type.

To investigate the downstream mechanism, the present study focused on the NF-κB pathway, a canonical downstream effector of TLR signaling (21,22). The IL-17A$^+$ γδT cells from the BA murine model exhibited elevated NF-κB p65 and p-NF-κB p65 levels compared with in γδT cells (Fig. 5G and H), confirming the activation of NF-κB signaling. NF-κB p65 upregulation may ensure sufficient substrate availability for phosphorylation, whereas increased p-NF-κB

p65 indicates functional activation, consistent with previous reports on NF-κB signaling regulation (28,29). The co-culture system of *Tlr2*$^{-/-}$ or *Tlr4*$^{-/-}$ γδT cells with RRV-stimulated BECs or macrophages exhibited attenuated NF-κB activation, as evidenced by reduced levels of NF-κB p65 and p-NF-κB p65 compared with those in WT γδT cells (Fig. 6C-E). After stimulation of γδT cells with HMGB1 released by RRV-infected BECs or macrophages, the IL-17A level was significantly increased compared with that from BECs or macrophages uninfected with RRV (Fig. 4F). However, these effects were abolished by pretreatment with the NF-κB inhibitor Bay 11-7082 (Fig. 6F and G), demonstrating that HMGB1-TLR2/4 signaling depends on NF-κB to activate IL-17A$^+$ γδT cells.

Discussion

The present study demonstrated the key role of the HMGB1-TLR2/4-NF-κB axis in IL-17A$^+$ γδT cell activation in BA (Fig. 7). HMGB1, a pro-inflammatory cytokine, can be released by RRV-infected BECs and macrophages in BA; this activates IL-17A$^+$ γδT cells via TLR2/4-NF-κB signaling to produce IL-17A, which contributes to the inflammatory response. The present study provides novel insights into the activation of IL-17A$^+$ γδT cells in BA.

The IL-17 cytokine family members have various biological functions, including immunoprotective and inflammation-inducing processes. IL-17 is expressed in all cell types in the liver, highlighting the importance of the regulatory function of the IL-17 axis (8,10). The first identified member, IL-17A, is a key pathogenic cytokine in a variety of autoimmune and inflammatory diseases, and can be produced by CD4$^+$ and CD8$^+$ T cells, γδT cells and various innate immune cell populations (30-33). Several studies have reported the upregulation of hepatic IL-17A expression in BA, which is associated with bile duct inflammatory injury (7,8,10). Regarding the source of IL-17A, Th17 cells are considered to be a notable contributor (7,8); however, there are also reports suggesting that γδT cells are the exclusive source of IL-17A in experimental BA (9,10). The present study revealed that hepatic IL-17A expression was upregulated in patients with BA, which is consistent with previous reports. IL-17A was mainly generated by γδT and Th17 cells. Notably, after inhibiting the secretion of IL-17A in γδT and Th17 cells, it was demonstrated that γδT cells contributed more to IL-17A production, suggesting that γδT cells are the major producers of IL-17A.

γδT cells are an important subset of innate immune T cells that function between innate and adaptive immunity, and serve a vital role in immunomodulatory responses in newborns (34,35). These cells can produce abundant cytokines (including IL-17A) that trigger rapid immune responses in infection, inflammation and autoimmune diseases (34,36). Moreover, γδT cells have innate receptor expression combined with IL-17A production, making them the first line of defense, and IL-17A$^+$ γδT cells can differentiate and develop in a way that is different from Th17 cells to rapidly respond to pathogen invasion (36-38). In the present study, the hepatic IL-17A$^+$ γδT cells in the BA murine model increased from day 3 and reached a peak on day 7, confirming their importance in IL-17A production and proinflammation in the early phase of BA. This finding is similar to the results of previous reports, which reported that Th17 cells begin to secrete IL-17A on day 8 of RRV-induced experimental BA to promote biliary inflammation (8,39). The present findings extend this paradigm by demonstrating that γδT cells precede Th17 cells in driving IL-17A-dependent inflammation during early phases, whereas Th17 cells dominate in later phases. Knocking out the *Tcrδ* gene reduced BA incidence and alleviated inflammation in the biliary system, whereas the condition worsened after adoptive transfusion of IL-17A$^+$ γδT cells, highlighting the contribution of IL-17A$^+$ γδT cells in inducing inflammatory destruction of the biliary system in BA. However, the mechanism underlying activation of IL-17A$^+$ γδT cells remains to be elucidated.

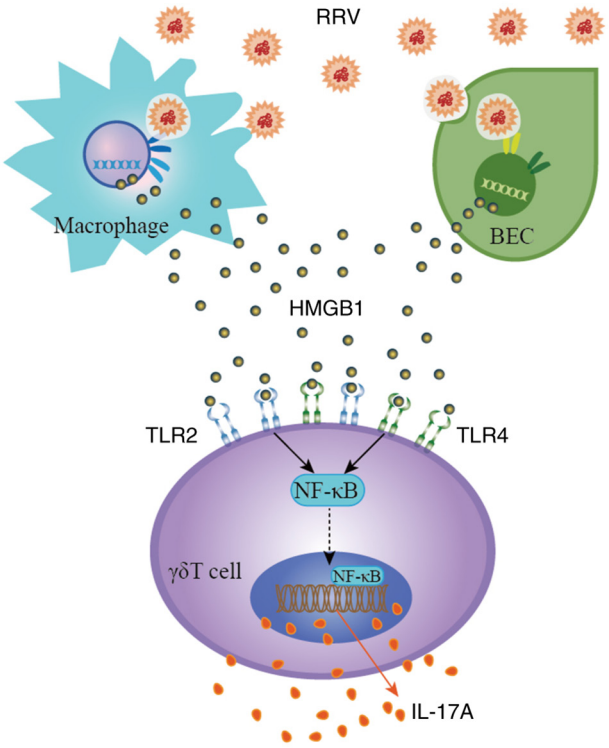

Figure 7. Schematic diagram showing the mechanism of activation of IL-17A$^+$ γδT cells mediating inflammatory injury in biliary atresia. BEC, biliary epithelial cell; HMGB1, high-mobility group box-1; RRV, rhesus rotavirus; TLR, Toll-like receptor.

DAMPs have been reported to mediate persistent inflammatory injury by activating innate immune responses, and HMGB1, which is passively released by injured BECs, can act as a DAMP, alerting the immune system and triggering an immediate response during tissue injury (13,40,41). HMGB1 has been shown to be upregulated in BA and serves a pivotal role in its pathogenesis (13,14). Consistent with this, the present study detected a significant increase in hepatic HMGB1 levels in human and experimental BA. Notably, inhibition of HMGB1 by glycyrrhizin reduced hepatic IL-17A$^+$ γδT cells and IL-17A levels, and alleviated inflammation of the biliary system in the early stage of experimental BA, suggesting that HMGB1 is required for IL-17A$^+$ γδT cell activation in BA. The increase in IL-17A$^+$ γδT cells after HMGB1 stimulation of hepatic γδT cells *in vitro* further supported the perspective that HMGB1 is a direct driver of γδT cell activation. This is similar to the previously reported positive role of HMGB1 in the activation of IL-17A$^+$ γδT cells in acetaminophen-induced liver inflammation (11).

Subsequently, the present study analyzed the source of HMGB1 in BA. *In vitro* studies demonstrated that HMGB1 could be released by BECs and macrophages infected with RRV, which are the main target cells of RRV infection in BA (20,42). Previous studies have demonstrated that RRV-infected BECs in experimental BA can release a large amount of HMGB1 via active release function (13,25). The present study further verified that macrophages are important contributors to HMGB1 secretion in BA by detecting reductions in HMGB1 after depleting macrophages with $GdCl_3$. Notably, in addition to BECs and macrophages being the primary sources of HMGB1, other immunocytes near the hepatic portal area may also produce HMGB1, which requires further study.

BECs and macrophages may also secrete various other cytokines in addition to HMGB1 to participate in IL-17A$^+$ γδT cell activation under RRV infection. Therefore, the present study established a co-culture system of BECs or macrophages and γδT cells, and revealed that IL-17A levels were increased after RRV infection with BECs or macrophages and decreased after inhibition of HMGB1. These findings validated that the release of HMGB1 from RRV-infected BECs and macrophages is directly involved in the IL-17A production by γδT cells.

TLRs recognize endogenous DAMPs and exogenous PAMPs to initiate signal transduction, thereby stimulating the production of various cytokines to trigger an inflammatory response, and HMGB1 is a well-known powerful stimulating ligand of TLRs (20,43). γδT cells have been reported to express TLRs and regulate the early immune response against different pathogens (44,45), and TLR2 and TLR4 serve an irreplaceable innate role in enhancing γδT cell activation to generate IL-17A in various pathological states (27,44,45). TLR2 and TLR4 levels have been reported to be increased on multiple types of cells during modulation of the immune reaction to RRV infection (20,46). Notably, the HMGB1-TLR4 interaction has been reported to amplify NF-κB-driven inflammation in sepsis and autoimmune diseases (47,48), suggesting a conserved pathway across pathologies. Therefore, it was hypothesized that HMGB1 may mediate the activation of γδT cells to produce IL-17A through the TLR2/4-NF-κB axis in BA. Supporting this, hepatic TLR2 and TLR4 expression levels were elevated in BA, with upregulated TLR2 and TLR4 detected on the surface of hepatic IL-17A$^+$ γδT cells, indicating that the TLR2 and TLR4 signaling pathways of IL-17A$^+$ γδT cells were activated during inflammatory injury. Moreover, the activation of IL-17A$^+$ γδT cells induced by HMGB1 was blocked through TLR2/4 knockout, confirming pathway dependency. These findings demonstrated that HMGB1-TLR2/4 signaling pathways mediate the activation of IL-17A$^+$ γδT cells to participate in the inflammatory injury of BA. A previous study demonstrated that γδT cells can express TLRs to contribute to early immune response in pathological conditions (44). By contrast, a deficiency of TLR2 has been shown to reduce the immune response of γδT cells in mice after native lipid A injection, whereas co-stimulation with TLR2 and IL-23 could promote the generation of IL-17 in γδT cells (49,50). In addition, TLR4 is important in promoting the activation of γδT cells, which respond to lipopolysaccharide in a TLR4-dependent manner (51). TLR4 is involved in the activation of IL-17A$^+$ γδT cells via the HMGB1-TLR4-IL-23 axis in macrophages (11). These studies also support the current findings on the importance of TLR2 and TLR4 in HMGB1-mediated IL-17A$^+$ γδT cell activation. Notably, in addition to TLR2 and TLR4, other receptors of HMGB1 may be involved in stimulating the generation of inflammatory cytokines such as IL-17A, causing inflammatory injury of BA, which requires further investigation. HMGB1 could interact with multiple pattern recognition receptors other than TLR2 and TLR4, such as the receptor for advanced glycation end products (RAGE), and serves a critical role in various pathologies (52-54). The present study focused on TLR2 and TLR4 given their well-documented expression on γδT cells and supported role in γδT cell activation across different pathologies (11,42,49-52). By contrast, the expression and functional relevance of RAGE specifically in γδT cells remain to be elucidated, presenting a potential direction for future research (55). Notably, the present discovery of NF-κB as the downstream effector of HMGB1-TLR2/4 signaling in the activation of IL-17A$^+$ γδT cells expands upon the aforementioned work. This finding was consistent with the classical role of NF-κB in TLR signaling (47,48), which may be a key regulator of γδT cell differentiation toward the IL-17A phenotype.

In conclusion, the present study indicated that HMGB1 released by RRV-infected BECs and macrophages in BA could activate IL-17A$^+$ γδT cells to produce IL-17A via the HMGB1-TLR2/4-NF-κB axis, triggering the inflammatory response of the biliary system in BA. Novel therapies targeting the HMGB1-TLR2/4-NF-κB axis may reduce IL-17A$^+$ γδT cell activation, inhibiting the inflammatory injury of BA.

Acknowledgements

Not applicable.

Funding

The present study was supported by the National Natural Science Foundation of China (grant no. 81670511) and the Natural Science Research Project of Science and Technology Department of Shanxi Province (grant no. 202303021211237).

Availability of data and materials

The data generated in the present study may be requested from the corresponding author.

Authors' contributions

MXZ, JFT, MH, YY, YZ, SQC, LYR, GQC, XZ, STT and JXZ designed the study and conceived the experiments. MXZ, JFT, MH and YY contributed to data collection, data analysis and drafting the manuscript. YZ, SQC, LYR, GQC and XZ contributed to data collection and analytical supervision. MXZ, JFT, MH, YY, STT and JXZ confirm the authenticity of all the raw data. STT and JXZ provided administrative support. All authors have read and approved the final manuscript.

Ethics approval and consent to participate

The present study was approved by the Ethics Committee of Union Hospital, Tongji Medical College, Huazhong University of Science and Technology (approval no. 2016-LSZ-S180) and

Shanxi Children's Hospital (approval no. 2RB-SB-2021-005), registered in the Chinese Clinical Trial Registry (registration ID: ChiCTR2000039619), and carried out in accordance with The Declaration of Helsinki. All animal experiments were approved by the Institutional Animal Care and Use Committee of Tongji Medical College, Huazhong University of Science and Technology (2024 IACUC no. 4296). Written informed consent was obtained from the guardians of all participants.

Patient consent for publication

Not applicable.

Competing interests

The authors declare that they have no competing interests.

References

1. Bezerra JA, Wells RG, Mack CL, Karpen SJ, Hoofnagle JH, Doo E and Sokol RJ: Biliary atresia: Clinical and research challenges for the twenty-first century. Hepatology 68: 1163-1173, 2018.
2. Tam PKH, Wells RG, Tang CSM, Lui VCH, Hukkinen M, Luque CD, De Coppi P, Mack CL, Pakarinen M and Davenport M: Biliary atresia. Nat Rev Dis Primers 10: 47, 2024.
3. Bessho K and Bezerra JA: Biliary atresia: Will blocking inflammation tame the disease? Annu Rev Med 62: 171-185, 2011.
4. Davenport M, Muntean A and Hadzic N: Biliary atresia: Clinical phenotypes and aetiological heterogeneity. J Clin Med 10: 5675, 2021.
5. Lakshminarayanan B and Davenport M: Biliary atresia: A comprehensive review. J Autoimmun 73: 1-9, 2016.
6. Wang J, Xu Y, Chen Z, Liang J, Lin Z, Liang H, Xu Y, Wu Q, Guo X, Nie J, *et al*: Liver immune profiling reveals pathogenesis and therapeutics for biliary atresia. Cell 183: 1867-1883.e26, 2020.
7. Yang Y, Liu YJ, Tang ST, Yang L, Yang J, Cao GQ, Zhang JH, Wang XX and Mao YZ: Elevated Th17 cells accompanied by decreased regulatory T cells and cytokine environment in infants with biliary atresia. Pediatr Surg Int 29: 1249-1260, 2013.
8. Lages CS, Simmons J, Maddox A, Jones K, Karns R, Sheridan R, Shanmukhappa SK, Mohanty S, Kofron M, Russo P, *et al*: The dendritic cell-T helper 17-macrophage axis controls cholangiocyte injury and disease progression in murine and human biliary atresia. Hepatology 65: 174-188, 2017.
9. Möhn N, Bruni E, Schröder A, Frömmel S, Gueler F, Vieten G, Prinz I, Kuebler JF, Petersen C and Klemann C: Synthetic retinoid AM80 inhibits IL-17 production of gamma delta T cells and ameliorates biliary atresia in mice. Liver Int 40: 3031-3041, 2020.
10. Klemann C, Schröder A, Dreier A, Möhn N, Dippel S, Winterberg T, Wilde A, Yu Y, Thorenz A, Gueler F, *et al*: Interleukin 17, produced by γδ T cells, contributes to hepatic inflammation in a mouse model of biliary atresia and is increased in livers of patients. Gastroenterology 150: 229-241.e5, 2016.
11. Wang X, Sun R, Wei H and Tian Z: High-mobility group box 1 (HMGB1)-Toll-like receptor (TLR)4-interleukin (IL)-23-IL-17A axis in drug-induced damage-associated lethal hepatitis: Interaction of γδ T cells with macrophages. Hepatology 57: 373-384, 2013.
12. Mohanty SK, Donnelly B, Temple H, Mowery S, Poling HM, Meller J, Malik A, McNeal M and Tiao G: Rhesus rotavirus receptor-binding site affects high mobility group box 1 release, altering the pathogenesis of experimental biliary atresia. Hepatol Commun 6: 2702-2714, 2022.
13. Mohanty SK, Donnelly B, Temple H, Ortiz-Perez A, Mowery S, Lobeck I, Dupree P, Poling HM, McNeal M, Mourya R, *et al*: High mobility group box 1 release by cholangiocytes governs biliary atresia pathogenesis and correlates with increases in afflicted infants. Hepatology 74: 864-878, 2021.
14. Ye CJ, Wang J, Yang YF, Shen Z, Chen G, Huang YL, Zheng YJ, Dong R and Zheng S: Upregulation of high mobility group box 1 may contribute to the pathogenesis of biliary atresia. Eur J Pediatr Surg 29: 388-393, 2019.
15. Venereau E, Casalgrandi M, Schiraldi M, Antoine DJ, Cattaneo A, De Marchis F, Liu J, Antonelli A, Preti A, Raeli L, *et al*: Mutually exclusive redox forms of HMGB1 promote cell recruitment or proinflammatory cytokine release. J Exp Med 209: 1519-1528, 2012.
16. Iwasaki A and Medzhitov R: Toll-like receptor control of the adaptive immune responses. Nat Immunol 5: 987-995, 2004.
17. Ren W, Zhao L, Sun Y, Wang X and Shi X: HMGB1 and Toll-like receptors: Potential therapeutic targets in autoimmune diseases. Mol Med 29: 117, 2023.
18. Kang R, Chen R, Zhang Q, Hou W, Wu S, Cao L, Huang J, Yu Y, Fan XG, Yan Z, *et al*: HMGB1 in health and disease. Mol Aspects Med 40: 1-116, 2014.
19. Saito T, Hishiki T, Terui K, Mitsunaga T, Terui E, Nakata M and Yoshida H: Toll-like receptor mRNA expression in liver tissue from patients with biliary atresia. J Pediatr Gastroenterol Nutr 53: 620-626, 2011.
20. Qiu Y, Yang J, Wang W, Zhao W, Peng F, Xiang Y, Chen G, Chen T, Chai C, Zheng S, *et al*: HMGB1-promoted and TLR2/4-dependent NK cell maturation and activation take part in rotavirus-induced murine biliary atresia. PLoS Pathog 10: e1004011, 2014.
21. Zhu D, Zou H, Liu J, Wang J, Ma C, Yin J, Peng X, Li D, Yang Y, Ren Y, *et al*: Inhibition of HMGB1 ameliorates the maternal-fetal interface destruction in unexplained recurrent spontaneous abortion by suppressing pyroptosis activation. Front Immunol 12: 782792, 2021.
22. Cheng Y, Xiong J, Chen Q, Xia J, Zhang Y, Yang X, Tao K, Zhang S and He S: Hypoxia/reoxygenation-induced HMGB1 translocation and release promotes islet proinflammatory cytokine production and early islet graft failure through TLRs signaling. Biochim Biophys Acta Mol Basis Dis 1863: 354-364, 2017.
23. Shivakumar P, Campbell KM, Sabla GE, Miethke A, Tiao G, McNeal MM, Ward RL and Bezerra JA: Obstruction of extrahepatic bile ducts by lymphocytes is regulated by IFN-gamma in experimental biliary atresia. J Clin Invest 114: 322-329, 2004.
24. Livak KJ and Schmittgen TD: Analysis of relative gene expression data using real-time quantitative PCR and the 2(-Delta Delta C(T)) method. Methods 25: 402-408, 2001.
25. Jafri M, Donnelly B, Allen S, Bondoc A, McNeal M, Rennert PD, Weinreb PH, Ward R and Tiao G: Cholangiocyte expression of alpha2beta1-integrin confers susceptibility to rotavirus-induced experimental biliary atresia. Am J Physiol Gastrointest Liver Physiol 295: G16-G26, 2008.
26. Park JS, Gamboni-Robertson F, He Q, Svetkauskaite D, Kim JY, Strassheim D, Sohn JW, Yamada S, Maruyama I, Banerjee A, *et al*: High mobility group box 1 protein interacts with multiple Toll-like receptors. Am J Physiol Cell Physiol 290: C917-C924, 2006.
27. Zuo A, Liang D, Shao H, Born WK, Kaplan HJ and Sun D: In vivo priming of IL-17(+) uveitogenic T cells is enhanced by Toll ligand receptor (TLR)2 and TLR4 agonists via γδ T cell activation. Mol Immunol 50: 125-133, 2012.
28. Mao H, Zhao X and Sun SC: NF-κB in inflammation and cancer. Cell Mol Immunol 22: 811-839, 2025.
29. Ghosh S and Hayden MS: New regulators of NF-kappaB in inflammation. Nat Rev Immunol 8: 837-848, 2008.
30. Mills KHG: IL-17 and IL-17-producing cells in protection versus pathology. Nat Rev Immunol 23: 38-54, 2023.
31. Langrish CL, Chen Y, Blumenschein WM, Mattson J, Basham B, Sedgwick JD, McClanahan T, Kastelein RA and Cua DJ: IL-23 drives a pathogenic T cell population that induces autoimmune inflammation. J Exp Med 201: 233-240, 2005.
32. McGeachy MJ, Cua DJ and Gaffen SL: The IL-17 family of cytokines in health and disease. Immunity 50: 892-906, 2019.
33. McGonagle DG, McInnes IB, Kirkham BW, Sherlock J and Moots R: The role of IL-17A in axial spondyloarthritis and psoriatic arthritis: Recent advances and controversies. Ann Rheum Dis 78: 1167-1178, 2019.
34. Muro R, Takayanagi H and Nitta T: T cell receptor signaling for γδT cell development. Inflamm Regen 39: 6, 2019.
35. Gibbons DL, Haque SFY, Silberzahn T, Hamilton K, Langford C, Ellis P, Carr R and Hayday AC: Neonates harbour highly active gammadelta T cells with selective impairments in preterm infants. Eur J Immunol 39: 1794-1806, 2009.
36. Xu L, Chen F, Fan W, Saito S and Cao D: The role of γδT lymphocytes in atherosclerosis. Front Immunol 15: 1369202, 2024.
37. Roark CL, Simonian PL, Fontenot AP, Born WK and O'Brien RL: gammadelta T cells: An important source of IL-17. Curr Opin Immunol 20: 353-357, 2008.

38. Martin B, Hirota K, Cua DJ, Stockinger B and Veldhoen M: Interleukin-17-producing gammadelta T cells selectively expand in response to pathogen products and environmental signals. Immunity 31: 321-330, 2009.
39. Liu YJ, Li K, Yang L, Tang ST, Wang XX, Cao GQ, Li S, Lei HY and Zhang X: Dendritic cells regulate Treg-Th17 axis in obstructive phase of bile duct injury in murine biliary atresia. PLoS One 10: e0136214, 2015.
40. Maher JJ: DAMPs ramp up drug toxicity. J Clin Invest 119: 246-249, 2009.
41. Nakano T, Goto S, Lai CY, Hsu LW, Kao YH, Lin YC, Kawamoto S, Chiang KC, Ohmori N, Goto T, *et al*: Experimental and clinical significance of antinuclear antibodies in liver transplantation. Transplantation 83: 1122-1125, 2007.
42. Mohanty SK, Ivantes CAP, Mourya R, Pacheco C and Bezerra JA: Macrophages are targeted by rotavirus in experimental biliary atresia and induce neutrophil chemotaxis by Mip2/Cxcl2. Pediatr Res 67: 345-351, 2010.
43. Yu M, Wang H, Ding A, Golenbock DT, Latz E, Czura CJ, Fenton MJ, Tracey KJ and Yang H: HMGB1 signals through toll-like receptor (TLR) 4 and TLR2. Shock 26: 174-179, 2006.
44. Wesch D, Peters C, Oberg HH, Pietschmann K and Kabelitz D: Modulation of γδ T cell responses by TLR ligands. Cell Mol Life Sci 68: 2357-2370, 2011.
45. Dar AA, Patil RS and Chiplunkar SV: Insights into the relationship between toll like receptors and gamma delta T cell responses. Front Immunol 5: 366, 2014.
46. Xu J, Yang Y, Wang C and Jiang B: Rotavirus and coxsackievirus infection activated different profiles of toll-like receptors and chemokines in intestinal epithelial cells. Inflamm Res 58: 585-592, 2009.
47. Wang J, Li R, Peng Z, Hu B, Rao X and Li J: [Corrigendum] HMGB1 participates in LPS-induced acute lung injury by activating the AIM2 inflammasome in macrophages and inducing polarization of M1 macrophages via TLR2, TLR4, and RAGE/NF-κB signaling pathways. Int J Mol Med 45: 1628, 2020.
48. Luo L, Wang S, Chen B, Zhong M, Du R, Wei C, Huang F, Kou X, Xing Y and Tong G: Inhibition of inflammatory liver injury by the HMGB1-A box through HMGB1/TLR-4/NF-κB signaling in an acute liver failure mouse model. Front Pharmacol 13: 990087, 2022.
49. Mokuno Y, Matsuguchi T, Takano M, Nishimura H, Washizu J, Ogawa T, Takeuchi O, Akira S, Nimura Y and Yoshikai Y: Expression of toll-like receptor 2 on gamma delta T cells bearing invariant V gamma 6/V delta 1 induced by Escherichia coli infection in mice. J Immunol 165: 931-940, 2000.
50. Deetz CO, Hebbeler AM, Propp NA, Cairo C, Tikhonov I and Pauza CD: Gamma interferon secretion by human Vgamma2Vdelta2 T cells after stimulation with antibody against the T-cell receptor plus the toll-like receptor 2 agonist Pam3Cys. Infect Immun 74: 4505-4511, 2006.
51. Reynolds JM, Martinez GJ, Chung Y and Dong C: Toll-like receptor 4 signaling in T cells promotes autoimmune inflammation. Proc Natl Acad Sci USA 109: 13064-13069, 2012.
52. Andersson U and Tracey KJ: HMGB1 is a therapeutic target for sterile inflammation and infection. Annu Rev Immunol 29: 139-162, 2011.
53. Sims GP, Rowe DC, Rietdijk ST, Herbst R and Coyle AJ: HMGB1 and RAGE in inflammation and cancer. Annu Rev Immunol 28: 367-388, 2010.
54. van Beijnum JR, Buurman WA and Griffioen AW: Convergence and amplification of toll-like receptor (TLR) and receptor for advanced glycation end products (RAGE) signaling pathways via high mobility group B1 (HMGB1). Angiogenesis 11: 91-99, 2008.
55. Wang Z, Zhou H, Zheng H, Zhou X, Shen G, Teng X, Liu X, Zhang J, Wei X, Hu Z, *et al*: Autophagy-based unconventional secretion of HMGB1 by keratinocytes plays a pivotal role in psoriatic skin inflammation. Autophagy 17: 529-552, 2021.